Pre-gelation staining expansion microscopy (PS-ExM) for visualisation of the *Plasmodium* liver stage

Kodzo Atchou[1,2,‡], Bianca Manuela Berger[1,2,‡], Volker Heussler[1,*] and Torsten Ochsenreiter[1,*]

[1]Institute of Cell Biology, University of Bern, Bern, Switzerland
[2]Graduate School for Cellular and Biomedical Sciences, University of Bern, Bern, Switzerland

*Authors for Correspondence: volker.heussler@unibe.ch, torsten.ochsenreiter@unibe.ch
‡Kodzo Atchou and Bianca Manuela Berger contributed equally to this work

Key words: *Plasmodium,* Liver-stage, Expansion Microscopy, Mitochondria, Lysosomes

Summary Statement

This protocol for investigating the *Plasmodium* liver stage involves the expansion of pre-stained samples, leading to a significantly expedited procedure, and enhanced preservation of specific epitopes.

Abstract

Fluorescence and light microscopy are important tools in the history of natural science. However, the resolution of microscopes is limited by the diffraction of light. One possible method to circumvent this physical restriction is the recently developed expansion microscopy (ExM). However, the original ultrastructure ExM (U-ExM) protocol is very time-consuming, and some epitopes are lost during the process. In this study, we developed a shortened pre-gelation staining ExM (PS-ExM) protocol and tested it to investigate the *Plasmodium* liver stage. The protocol presented in this study allows expanding pre-stained samples, which results in shorter incubation times, better preservation of some epitopes, and the advantage that non-expanded controls can be performed alongside using the same staining protocol. The protocol applicability was accessed throughout the *Plasmodium* liver stage, showing isotropic

five-fold expansion. Furthermore, we used PS-ExM to visualise parasite mitochondria as well as the association of lysosomes to the parasitophorous vacuole membrane (PVM) as an example of visualising host-pathogen interaction. We are convinced that this new tool will be helpful for a deeper understanding of the biology of the *Plasmodium* liver stage.

Introduction

Malaria is a debilitating and potentially fatal disease caused by *Plasmodium* parasites. It is a major global health issue, affecting millions of people in developing countries, particularly in sub-Saharan Africa (Snow et al., 2005; WHO, 2021). Despite extensive research efforts made, malaria remains a major public health challenge, and new treatment options are needed to effectively control and prevent the disease (Tse et al., 2019). A major challenge in the development of new effective anti-malaria drugs is the parasite's ability to rapidly develop resistance to antimalarial drugs (Plowe, 2022; White, 2004). The *Plasmodium* life cycle is complex consisting of both asexual and sexual stages that are present in the vertebrate host and in the mosquito. The transmission of malaria occurs when an infected female *Anopheles* mosquito bites a human and releases up to several 100 sporozoites into the skin (Amino et al., 2006; Beier, 1998; Venugopal et al., 2020). Sporozoites are motile and a proportion of them enter blood vessels and are transported with the blood flow to the liver where they invade hepatocytes (Tavares et al., 2013). Inside the liver cells, the parasite resides within a parasitophorous vacuole (PV), in which the parasite proliferates from one single sporozoite to thousands of daughter parasites, called merozoites. This process is also known as schizogony. The merozoites exit the liver cells in vesicles known as merosomes that are transported to adjacent blood vessels (Mota et al., 2001). When the merosomes rupture, they release the merozoites which subsequently invade erythrocytes. The liver stage represents a crucial opportunity for anti-malaria interventions since it is clinically silent. The characteristic symptoms of malaria only occur upon repeated rounds of asexual blood stage replication and the associated rupture of the red blood cell (Derbyshire et al., 2011; Vaughan & Kappe, 2017). In the infected red blood cells, some merozoites develop into gametocytes (Cowman & Crabb, 2006). Gametocytes are the sexual form of the

parasite which, when taken up during the blood meal of a mosquito, differentiate into gametes and mate in the midgut of the insect to form a zygote. This motile parasite stage transmigrates the midgut epithelium and forms a so-called oocyst, inside which sporozoites develop. Upon rupture of the oocyst, sporozoites migrate to the mosquito's salivary gland and can be transmitted to the next human host. An important tool for the discovery of new treatment options is a better understanding of molecular details of the parasite's life cycle and host-pathogen interactions. Conventional light microscopy allowed us to gain insight into cellular organisation (Rankin et al., 2010). However, due to the diffraction of light, the maximal resolution lies between 200-300 nm (Heintzmann & Ficz, 2006). Subcellular imaging of the parasite remains therefore challenging and requires super-resolution techniques such as PALM (photo-activated localization microscopy), STORM (stochastic optical reconstruction microscopy), SIM (structured illumination microscopy), and STED (stimulated emission depletion) (reviewed by Heintzmann and Ficz, 2006). However, they require expensive and complex microscopical equipment and special sample preparation (Heintzmann & Ficz, 2006). In comparison, the recently developed expansion microscopy (ExM) is relatively straightforward and does not require complicated preparations or specialised equipment, making it accessible to researchers all over the world (Chen et al., 2015; Gambarotto et al., 2019; Gao et al., 2017). In a relatively short period of time, ExM became a new cutting-edge imaging technique that has revolutionised the field of microscopy. The physical expansion of the sample results in a significant improvement in spatial resolution compared to traditional light microscopy techniques. Expansion microscopy is based on the usage of a hydrogel matrix. The hydrogel matrix is composed of a polymer network that is covalently attached to the biological sample and expands upon hydration (Chen et al., 2015). There are several different expansion microscopy protocols that have been developed, each with its own strengths and limitations (Chen et al., 2015; Gambarotto et al., 2021; Tillberg et al., 2016). The original ExM protocol developed by Edward Boyden's group in 2015 has been widely used and has been modified and improved over the years to increase the accuracy and specificity of the technique (Chen et al., 2015; Gao et al., 2017). Nevertheless, the basic principles of the protocol remain the same. One of the nowadays most widely used expansion microscopy protocols is ultrastructure expansion microscopy (U-ExM), which has been shown to preserve the cellular architecture in a near-native manner, achieving

a four-fold expansion (Gambarotto et al., 2019, 2021). In comparison to the original protocol from Edward Boyden's group, the staining is performed after (instead of before) embedding the sample in the swellable gel. The post-expansion staining reduces antibody competition through the decrowding of the epitopes and prevents fluorophore loss (Gambarotto et al., 2019). However, the protocol is time-consuming, requiring roughly two days. Since the antibody staining is performed on the gel, the incubation times are rather long with approximately three hours for each antibody incubation (Gambarotto et al., 2021). Another limitation is the loss of epitopes during the denaturation step. An alternative to the post-expansion labelling protocol is the proExM protocol developed by the group of Joshua Vaughan (Chozinski et al., 2016). Here, biological samples are stained with fluorescent antibodies before the gelation process begins. The fluorescent labels are afterwards covalently linked to the polymer. Subsequent protease treatment is used for exposing protein epitopes while preserving the signal of the quite protease-resistant fluorescent labels. This approach has the advantage that existing stained samples can be entered into the expansion process and non-expanded samples can be performed under the same conditions (Chozinski et al., 2016). Since its first application in 2015, the ExM has been applied to a variety of samples, including cells, tissues, and even entire organisms (Chen et al., 2015; Gao et al., 2017). Recently, the U-ExM was used to study the molecular architecture of *Plasmodium* gametocytes (Chozinski et al., 2016; Rashpa & Brochet, 2022). Furthermore, U-ExM allowed gaining insight into the asexual *Plasmodium* blood stage (Liffner & Absalon, 2021). The aim of the study was to optimise the ultrastructure ExM (U-ExM) protocol developed by Gambarotto et al. to study the *Plasmodium* liver stage (Gambarotto et al., 2019, 2021). With some major adaptations for pre-stained samples, we used this method to visualise different developmental stages of the *Plasmodium* liver stage. This fast and easy protocol will now allow researchers to gain a more detailed insight into the *Plasmodium* liver stage.

Results

Five-fold isotropic expansion of *Plasmodium* liver stage with pre-gelation staining expansion microscopy (PS-ExM).

The aim of this study was to adapt the ultrastructure expansion microscopy (U-ExM) protocol to investigate intracellular *Plasmodium* parasites during the liver stage development. The protocol developed by Gambarotto et al. in 2019 results in a near-native expansion of cultured cells (Gambarotto et al., 2019, 2021). In the original protocol, the antibody staining was performed after embedding the cells in a swellable gel, which resulted in a rather long antibody incubation time of about three hours. Furthermore, some epitopes were lost during the denaturation prior to the antibody staining. Additionally, the non-expanded controls had to be prepared separately. In this study, the original U-ExM protocol was modified to allow expansion of pre-stained specimens (pre-gelation staining ExM, PS-ExM). Overall, the reagents used for fixation (formaldehyde), anchoring (acrylamide), gelation, and denaturation were identical to the ones previously described for U-ExM (Gambarotto et al., 2019, 2021). However, the incubation time for each of the steps was strongly reduced to better preserve the fluorescent signal. A comparison between the original and the adapted PS-ExM protocol version is shown in Table 1.

An overview of the PS-ExM protocol is depicted in Fig. 1A, and the detailed description can be found in the methods section. Immunofluorescence assay was performed on infected HeLa cells. Primary and secondary antibody incubations were performed for one hour. In comparison, in the original U-ExM protocol, each antibody incubation took three hours (Table 1). The incubation time with formaldehyde and acrylamide was reduced to two hours compared to the original U-ExM protocol, in which the incubation lasted for five hours (Table 1). The addition of acrylamide results in functionalization of the cells and subsequently allows to chemically link the proteins into a polyacrylamide gel matrix. Gelation was performed for 30 min in comparison to 1.5 hours in the original protocol (Table 1). For isotropic expansion, the cells were denatured for 30 min, which is three times shorter compared to the original protocol (Table 1). DNA of host cells and the parasites was stained with DAPI. After gel expansion, the cells were imaged. A major challenge to studying the *Plasmodium* liver stage in expansion microscopy is to be able to expand the intracellular parasite as well as the host cell under the same conditions.

Representative images of non-expanded and expanded cells six hours post-infection (hpi) are depicted in Fig. 1B. The parasitophorous vacuole membrane (PVM) was stained with anti-UIS4 antibodies to identify infected HeLa cells. When comparing expanded and non-expanded cells, the morphological integrity of the PVM was preserved. The expansion factor measured was 5-fold for HeLa cell nuclei (Fig. 1C) and 5.1-fold for the parasite nuclei measured at 56 hpi (Fig. 1D). The PS-ExM protocol yielded isotropic expansion, as accessed through 3D sphericity measurements of parasite nuclei in both non-expanded and expanded samples (Supplementary Fig. S1A and B). The isotropic expansion of the PS-ExM protocol was determined using the trophozoite developmental stage, as the parasite has a single nucleus with a spheric appearance at this stage (Roques et al., 2023). Furthermore, microtubule (α-tubulin) staining demonstrated the preservation of the cell morphology in the PS-ExM protocol (Supplementary Fig. S1D). We compared the preservation of different epitopes between the original protocol and the adapted PS-ExM protocol: the epitopes of UIS4, LAMP1 (lysosome-associated membrane protein 1) and α-tubulin were adversely affected using the original protocol, whereas the PS-ExM protocol resulted in excellent preservation of epitopes (Supplementary Fig. S1C and D).

The pre-gelation staining expansion microscopy protocol allows for studying the interaction of *Plasmodium* liver stage parasites and host cell lysosomes.

During the *Plasmodium* liver stage, the parasite resides within a PV. The applicability of the PS-ExM was accessed for different phases of parasite liver stage development (Fig. 2A). The earliest time point was chosen as six hours post-infection where only one single parasite nucleus is visible in the infected HeLa cell. The sporozoite having a banana-like shape started being rounded at 24 hours post-infection but still had a single nucleus. At 30 hours post-infection, the parasite initiates the schizogony with massive replication which is visible at 48 and 56 hours post-infection with now many parasite nuclei (Fig. 2A). Subsequently, the parasites undergo merogony and the PVM is ruptured. This time point was not included in this study since the host cells detach from the coverslip at this phase. Besides being able to expand the whole *Plasmodium* liver stage, the applicability of the new PS-ExM to

study host-pathogen interaction was tested using antibodies that detect proteins of both, parasite and host cell. Previous studies showed the association of lysosomes to the PV (da Silva et al., 2012; Niklaus et al., 2019). The interaction of lysosomes with the PVM was investigated in greater detail with PS-ExM. LAMP1, a lysosome membrane marker, was used to stain host cell lysosomes and UIS4 antibody staining was performed to outline the PVM. As previously described, lysosomes were found in close proximity to the PVM (Niklaus et al., 2019) (Fig. 2B). The lysosome interaction with the PVM was investigated at different time points of parasite development (24 hpi, 30 hpi, and 48 hpi), as shown in Supplementary Fig. S2A and B. By utilising Imaris software, we measured the fusion of lysosomes with the PVM, revealing that 25% of host lysosomes were attached to the PVM in non-expanded cells, whereas this number increased to 35% in expanded cells (Supplementary Fig. S2C and D). We hypothesise that the improved staining achieved with the PS-ExM protocol contributes to this observed difference. In the PS-ExM samples, lysosomes appeared as vesicle-like structures, allowing for more accurate identification and quantification of lysosomes on the PVM compared to non-expanded controls, where lysosomes appeared as dots. The vesicle-like morphology of lysosomes provided valuable insights into the interaction between host cell lysosomes and the PVM (Fig. 3). We observed that the lysosome sizes varied at the early time point 6 hours post-infection (Fig. 3A). The host cells might attack the pathogen by engulfing parts of the parasite PVM into lysosomes for digestion. Imaging showed that some large lysosomes contain PVM structures (Fig. 3A, ROI1 and 2). At the contact sides of lysosomes with the PVM, we observed a weaker UIS4 signal, suggesting fusion of the two membranes and their components (Fig. 3A, ROI3). Once the parasite became established within the host cell at 48 hours post-infection, we observed a diffuse LAMP1 signal on the PVM (Fig. 3B, ROI1), again suggesting lysosome fusion with the PVM as previously described (Niklaus et al., 2019). Furthermore, we observed lysosomes either attached or fused to the PVM (Fig. 3C, ROI1-3). The fusion of the host lysosomes with the PVM resulted in a weaker UIS4 signal at the attachment point (Fig. 3C, ROI3) as observed at earlier time points of infection (Fig 3A, ROI3).

The pre-gelation staining expansion microscopy protocol effectively retains the integrity of mitochondrial networks.

To further evaluate the utility of the novel PS-ExM protocol in enhancing our understanding of parasite biology, we examined the preservation of mitochondria following expansion (Fig. 4). *Plasmodium* mitochondria were labelled with antibodies against *Toxoplasma gondii* heat shock protein 70 (TgHSP70), which also cross-reacts with *P. berghei* mitochondrial heat shock protein 70 (Eickel et al., 2013). We investigated mitochondrial development during the *Plasmodium* liver stage at various time points post-infection (6 hpi, 30 hpi, 48 hpi, and 56 hpi). Remarkably, the expansion process did not compromise the structural integrity of the parasite's mitochondrial network (Fig. 4, Supplementary Movie 1). Utilising the TgHSP70 signal, we generated a 3D model of the expanded mitochondrial network using Imaris software (Fig. 4). The parasite's mitochondria undergo extensive branching following hepatocyte invasion, ultimately distributing within the forming merozoites as previously described (Stanway et al., 2011).

Discussion

In this study, U-ExM was used for the first time to investigate *Plasmodium* liver stage parasites. The protocol originally developed by Gambarotto et al. was adapted to be used on pre-stained *Plasmodium*-infected HeLa cells (Gambarotto et al., 2019, 2021). While using the same chemical approach as in the U-ExM protocol, we performed a pre-expansion staining ExM (PS-ExM). Importantly, the time required for the U-ExM protocol was approximately halved from two to one day of work. In the original protocol developed by Gambarotto et al., the antibody incubation times were rather long, with three hours per incubation (Gambarotto et al., 2021). Performing the staining on cells prior to gelation allows for reducing the incubation time to one hour. Furthermore, non-expanded controls can be performed simultaneously using the same staining protocol as the expanded samples.

With the new PS-ExM protocol, both the host cell as well as the developing parasite exhibited isotropic five-fold expansion throughout the entire *Plasmodium* liver stage (Fig.1). We evaluated the effectiveness of the PS-ExM protocol in preserving

epitopes by staining the parasite vacuole membrane (UIS4), host lysosomes (LAMP1), and parasite mitochondria (TgHSP70). In comparison to the original protocol, the PS-ExM protocol demonstrated superior preservation of the UIS4 and LAMP1 epitopes (Supplementary Fig. S1C and D). Additionally, the structural integrity of the parasite's mitochondrial networks was maintained throughout the liver stage expansion, as depicted in Fig. 4. In summary, the PS-ExM protocol provides excellent preservation of parasite mitochondria, the PVM, and host lysosomes, making it a valuable tool for in-depth organelle studies. By using α-tubulin to delineate single-cell borders for quantifying lysosome attachment to the PVM, we also observed that the PS-ExM protocol better preserved microtubules compared to the original protocol (Supplementary Fig. S1D). These results suggest that, as compared to the original protocol, the PS-ExM maintains epitopes more effectively. This might be due to epitope loss during the denaturation time in the U-ExM protocol, which has been previously observed for some epitopes (Chozinski et al., 2016; Gao et al., 2017; Tillberg et al., 2016). By performing the antibody staining at the beginning of the protocol, this problem was solved. Additionally, as previously described, the antibodies themselves are linked to the swellable hydrogel during the acrylamide treatment potentially enhancing the antibody signal (Gao et al., 2017).

Additionally, the PS-ExM was used to investigate the host-pathogen interaction of lysosomes on the PVM. The lysosomes were seen as vesicle-like structures, and further details of the interaction between lysosomes and the parasite PVM were observed using the PS-ExM protocol (Fig. 2 and 3). Therefore, this novel protocol might be a helpful tool for further research of the molecular processes underlying the fusion of lysosomes to the parasite PVM.

However, expanding and imaging whole HeLa cells for quantitative purposes results in huge data sets (after deconvolution, a single image was around 10 GB for wide-field images, and for every experiment, at least ten images were acquired). Here, data storage and processing must be considered. Taken together, the PS-ExM protocol is faster compared to the original protocol, and it might be better suited for some epitopes that are otherwise lost during denaturation. The protocol here described can be further used to study host-pathogen interactions and gain further insight into the *Plasmodium* liver stage.

Materials and Methods

Ethics statement

Mice were obtained from Harlan Laboratories or Charles River. All mice (C57BL/6 and BALB/c) were maintained and bred in the central animal facility of the University of Bern. Studies were strictly performed under the guidelines and laws of the Animal Research Ethics Committee of the Canton of Bern, Switzerland (Permit Number: BE98/19) and the University of Bern Animal Care and Use Committee Switzerland. The mice were between six and 26 weeks old.

Mosquito maintenance

Mosquitoes were maintained inside stock cages in the insectarium at the Institute of Cell Biology of the University of Bern. Briefly, mosquitoes were fed with blood by placing a petri dish closed with parafilm containing the blood upside-down onto the mosquito cage. Blood was kept warm with a small Erlenmeyer containing hot water that was put on top of the petri dish. The mosquitoes were allowed to feed for 30 to 40 minutes before the petri dish containing the blood was removed. Two days after the feed, a beaker with water and filter paper was added to the mosquito cage to collect the mosquito eggs. The next day, the eggs were collected, washed once with 70% ethanol, and twice with water before being added to a metal bowl with a drop of about 10 µl of NobilFluid Artemia (JBL 33801 Germany), where they developed into larvae. After two days in the metal bowl, the larvae were transferred to a water-containing plastic bowl and fed with grounded Tetra TabiMin complete food tablets (Olibetta, 400080, Germany). Seven days later, the first pupae were collected and put in a stock cage, where they were kept at 27°C and 80% humidity until hatching. Adult mosquitoes were fed with 8% fructose supplemented with 0.2% PABA (Sigma-Aldrich, Cat. No. 100536). After 2 days, the female *Anopheles stephensi* mosquitoes were ready to be infected with *Plasmodium berghei* parasites.

Parasite maintenance in mosquitoes

A blood stabilate of the *P. berghei* ANKA strain expressing cytosolic mCherry under the Hsp70 promoter (Burda et al., 2015) was injected intraperitoneally into a naïve

Balb/c mouse. When the mouse reached a parasitemia of 3 to 5%, 50 µl of its infected blood was diluted with 150 µl 1X phosphate-buffered saline (PBS) and injected intravenously into a new mouse that was intraperitoneally injected with 200 µl phenylhydrazine (6 mg ml^{-1} in PBS, Sigma-Aldrich, 114715) three days prior to infection. After three days, 5 µl of blood was collected from the mouse tail and diluted in 500 µl of 1X PBS to check the parasitemia with fluorescence-activated cell sorting (FACS). When the mouse reached a parasitemia of 5% with at least 0.5% to 1% of gametocytes, the mouse was anaesthetized and used to feed 100–150 female *Anopheles stephensi* mosquitoes for 1 h. Infected mosquitoes were kept at 20.5°C and 80% humidity and fed with 8% fructose containing 0.2% PABA for 16 to 26 days for their salivary gland dissection and mammalian HeLa cell infection.

Mammalian cell culture and Infection

Human epithelial HeLa cells (European Cell Culture Collection) were maintained at 37°C with 5% CO_2. They were grown in minimum essential medium (MEM, BioConcept, 1-31F01-I) supplemented with Earle's salts and 10% heat-inactivated fetal calf serum (FCS, GE Healthcare) referred to as completed culture MEM. Medium contained 1% L-glutamine (Bioconcept, 5-10K00-H) and 1% penicillin/streptomycin (Bioconcept, 4-01F00-H. Cells were split every four days by treatment with accutase (Sigma-Aldrich, A6964). 40'000 HeLa cells were seeded on a coverslip in a 24-well plate (Greiner Bio-one, 662160) containing completed culture MEM. The next day, when the infected female *Anopheles stephensi* mosquitoes were between days 16 and 26 post-infection, the mosquitoes were anaesthetized with chloroform vapour (Merck, 67663 Germany) for about 20 seconds. Anaesthetized mosquitoes were briefly dipped into 70% ethanol and then transferred to 1X PBS. The mosquitoes were then put into 200 µl of non-supplemented MEM medium, referred to as infection medium, on a slide, and the head was then meticulously removed using surgical forceps. The two sets of each of the three salivary gland lobes were isolated from the head and transferred into an Eppendorf tube containing 20 µl of infection medium. The salivary glands that had been dissected were kept on ice until infection. The sporozoite parasites were mechanically released from the salivary glands using a pestle (Sigma-Aldrich, Z359947) that was powered by a cordless motor (Sigma-Aldrich, Z359971) with 10

pulses of 1-2 seconds. To determine the number of sporozoites, 10 µl of the infection medium was introduced to a Neubauer chamber. The seeded HeLa cells were then infected by the addition of 20'000 sporozoites in 200 µl. The 24-well plate was spun at 1000g for 1 minute to allow the sporozoites to settle quickly before being incubated at 37°C with 5% CO_2 for two hours. To get rid of mosquito salivary gland debris and sporozoites that failed to infect Hela cells, cells were washed twice with 500 µl of pre-warmed completed culture medium. Following that, cells were then incubated with 1 ml of completed culture medium at 37°C with 5% CO2 as previously described (Kaiser et al., 2017). The medium was exchanged with the cells at 24 and 48 hours post-infection. At specific time points after infection (6 hpi, 24 hpi, 30 hpi, 48 hpi, and 56 hpi), the cells were fixed and kept at 4°C for the immunofluorescence assay.

Immunofluorescence Assay

Infected HeLa cells were fixed with 4% paraformaldehyde (PFA) in PBS for 10 minutes at room temperature and subsequently washed twice with 1X PBS. Cells were permeabilized with 0.05% Triton (Fluka Chemie, T8787) for 5 minutes at room temperature, supplemented with 0.1% saponin (for washing out cytoplasmic background when staining lysosomes). Nonspecific antibody binding was reduced by blocking with 10% FCS in PBS for 20 minutes at room temperature. Subsequently, the cells were incubated with primary antibodies diluted in 10% FCS for 1 hour at room temperature. The primary antibodies used were: anti-UIS4 rabbit (P-Sinnis, Baltimore, 1:1000 in PS-ExM and 1:500 in post-staining ExM), anti-UIS4 chicken (Produced by Proteogenix in 2021, 1:1000), anti-LAMP1 mouse (Developmental Hybridoma Bank, clone H4A3, 1:1000 in PS-ExM and 1:500 in post-staining ExM), anti-TgHSP70 rabbit (Gift from Dominique Soldati Favre, 1:500) and anti-α-tubulin guinea pig (Geneva Antibody Facility, AA345, 1:200 in PS-ExM and 1:125 in post-staining ExM). The cells were then washed three times for 5 minutes each with 1X PBS and incubated with secondary antibodies at room temperature for 1 hour, protected from light. The secondary antibodies used were: anti-rabbit ATTO 647 (SIGMA, 40839, 1:1000 in PS-ExM and 1: 500 in post-staining ExM), anti-mouse Alexa Fluor 488 (Invitrogen Molecular Probes, A11001, 1:1000 in PS-ExM and 1:500 in post-staining ExM), anti-guinea pig Alexa Fluor 594 (Invitrogen Molecular Probes,

A11076, 1:1000 in PS-ExM and 1:500 in post-staining-ExM) and anti-chicken Alexa Fluor 594 (Invitrogen Molecular Probes, A11042, 1: 500). All antibodies are additionally listed in Supplementary Table S1. For non-expanded samples, the coverslips were stained with DAPI (SIGMA, D9542, 1:100) for 5 minutes before being mounted with 5 µl ProLong^{TM} Gold Antifade Mountant (Invitrogen, P36930). Images were acquired as described below.

Pre-gelation staining expansion microscopy (PS-ExM)

The chemical approach used was based on the U-ExM protocol published by Gambarotto et al. (Gambarotto et al., 2019, 2021). The protocol was optimized to make it applicable for pre-gelation-stained samples. The incubation times were shortened to better preserve the fluorophores of the pre-stained sample. Infected HeLa cells were stained as described above and samples were kept protected from light until imaging. Cells were incubated in PBS containing 0.7% formaldehyde (FA, 36.5–38%, F8775, SIGMA) and 1% acrylamide (AA, 40%, A4058, SIGMA). The latter will link the cells to the polymer during gelation. Compared to the original U-ExM protocol (5 h incubation), the formaldehyde and acrylamide incubation time was shortened to 1.5 h at 37°C. Subsequently, gelation was performed as described by Gambarotto et al. Gelation solution was prepared freshly: 0.5% ammonium persulfate (APS, 17874, ThermoFisher) and 0.5% tetramethylethylenediamine (TEMED, 17919, ThermoFisher) were added to the monomer solution containing 19% sodium acrylate (SA, 97–99%, 408220, SIGMA), 10% acrylamide (AA, 40%, A4058, SIGMA) and 0.1% N,N'-methylenebisacylamide (BIS, 2%, M1533, SIGMA). Per cover slip, 35 µl gelation solution were used. After incubating the sample on ice for 5 min, the gelation was carried out for 30 min at 37°C. Subsequently, gels were incubated in 1 ml denaturation buffer (200 mM sodium dodecyl sulfate SDS, 200 mM NaCl and 50 mM Tris in deionized water, pH 9) with gentle agitation at room temperature for 15 min to detach the gel from the cover slip. Denaturation was carried out at 95°C in denaturation buffer for 30 min. Gels were briefly incubated in PBS and afterwards, the DNA was stained with 5 µg ml^{-1} 4′,6-diamidino-2-phenylindole (DAPI, D9542-5MG, SIGMA) diluted in 2% bovine serum albumin (BSA) at 37°C with gentle agitation for one hour. Samples were expanded in deionized water for one hour. If the sample was imaged a day after expansion, the

gel was incubated in 0.2% propyl gallate (02370, SIGMA) to avoid photobleaching of samples until imaging. The chemicals are additionally listed in Supplementary Table S2.

Mounting and image acquisition

After the final expansion in deionized water, the gels were cut and mounted on poly-D-lysine (A38904, Gibco) functionalized 35 mm glass-bottom dishes (D35-20-1.5-N, Cellvis, 35 mm glass bottom dish with 20 mm micro-well #1.5 cover glass). These closed sample holders strongly reduced evaporation and shrinkage of the gels. All images were acquired with a 60x oil objective (NA= 1.4). The NIKON Ti 2 CREST V3 equipped with a Hamamatsu Flash 4.0 camera and a celesta light engine was used in widefield or spinning disc. Images were acquired with a z-step size of 300 nm and pixel size of 108 nm. Images acquired in wide field mode were deconvolved with Huygens Professional version [Huygens Remote Manager v3.8] (Scientific Volume Imaging, The Netherlands, http://svi.nl).

Image analysis

The open-source ImageJ platform was used to measure cell nuclei to determine the expansion factor (Schindelin et al., 2012). To measure parasite expansion, parasite nuclei were measured at 56 hpi. In comparison, minimal HeLa cell diameter was determined at different time points after infection. The expansion factor was calculated by dividing the average nuclear diameter of expanded cells by the average nuclear diameter of non-expanded samples. The 3D and 4D image analysis software Imaris (Imaris X64, 9.9.0 [Mar 11, 2022]) was used to segment parasite mitochondria and nuclei (Fig.3) and the lysosome attachment to the parasite PVM (Fig. S2). Briefly, to measure the lysosome attached to the parasite PVM in infected HeLa cells, the PVM (stained with anti-UIS4) was used to generate the isosurface, and the lysosomal vesicles (stained with LAMP1) were used to generate isospots. The generation of the isosurface from the anti-UIS4 staining was carried out using an isosurface detail value of 0.215 for non-expanded and expanded PVM in conjunction with the absolute intensity. The lysosome isospots were derived in the "local

contrast" mode using the estimated Point Spread Function (PSF). For non-expanded lysosomes, an estimated XY diameter of 0.4 µm and an estimated Z diameter of 0.5 µm were used, while for expanded lysosomes, an estimated XY diameter of 1.5 µm and 2.4 µm of estimated Z diameter were used. The isospots attached to the PVM were classified using the "Shortest Distance to Surfaces" parameter, with the threshold set at 0 µm distance to the PVM. The isospots within infected HeLa cells were manually selected based on anti-α-tubulin staining, which was used to delimitate the single-cell border. The isospots of non-infected HeLa cells were excluded from the analysis. Isospot numbers as well as the shortest distance to surfaces and isosurface data were exported into a Microsoft Excel file. The proportion of LAMP1 isospots attached to the PVM was calculated by dividing the number of LAMP1 isospots attached to the PVM by the total number of LAMP1 isospots within the infected cell. The Imaris software was also used to compute the isosurface of parasite nuclei in acquired z-stack images similar to the PVM isosurface details to determine isotropic expansion by measuring the sphericity of the nuclei in non-expanded and expanded samples. The data were structured and analysed using GraphPad Prism version 9.0.0 for Mac, GraphPad Software, San Diego, California, USA, www.graphpad.com. Statistical analysis was performed using the student's t test. *** P <0.001; ** P <0.01; * P <0.05.

Acknowledgment

We are grateful to Dominique Soldati for the anti-TgHSP70 antiserum. The authors acknowledge Ruth Rehmann, Ado Crnovrsanin, Clirim Jetishi, and Dr. Sandro Käser for discussions. The authors gratefully acknowledge Christin Berger for her assistance in revising the manuscript. Microscopy was performed on equipment supported by the Microscopy Imaging Center (MIC) of the University of Bern, Switzerland.

Competing interests

No competing interests declared.

Funding

This work was supported by the Swiss National Science Foundation (SNSF) (grant number 310030_182465) to Volker Heussler and (SNSF, 207525) to Torsten Ochsenreiter.

Data availability

All relevant data can be found within the article and its supplementary information.

References

Amino, R., Thiberge, S., Martin, B., Celli, S., Shorte, S., Frischknecht, F., & Ménard, R. (2006). Quantitative imaging of Plasmodium transmission from mosquito to mammal. *Nature Medicine*, *12*(2), 220–224. https://doi.org/10.1038/nm1350

Beier, J. C. (1998). MALARIA PARASITE DEVELOPMENT IN MOSQUITOES. *Annual Review of Entomology*, *43*(1), 519–543. https://doi.org/10.1146/annurev.ento.43.1.519

Burda, P.-C., Roelli, M. A., Schaffner, M., Khan, S. M., Janse, C. J., & Heussler, V. T. (2015). A Plasmodium Phospholipase Is Involved in Disruption of the Liver Stage Parasitophorous Vacuole Membrane. *PLOS Pathogens*, *11*(3), e1004760-. https://doi.org/10.1371/journal.ppat.1004760

Chen, F., Tillberg, P. W., & Boyden, E. S. (2015). Expansion microscopy. *Science*, *347*(6221), 543–548. https://doi.org/10.1126/science.1260088

Chozinski, T. J., Halpern, A. R., Okawa, H., Kim, H.-J., Tremel, G. J., Wong, R. O. L., & Vaughan, J. C. (2016). Expansion microscopy with conventional antibodies and fluorescent proteins. *Nature Methods*, *13*(6), 485–488. https://doi.org/10.1038/nmeth.3833

Cowman, A. F., & Crabb, B. S. (2006). Invasion of Red Blood Cells by Malaria Parasites. *Cell*, *124*(4), 755–766. https://doi.org/https://doi.org/10.1016/j.cell.2006.02.006

da Silva, M., Thieleke-Matos, C., Cabrita-Santos, L., Ramalho, J. S., Wavre-Shapton, S. T., Futter, C. E., Barral, D. C., & Seabra, M. C. (2012). The Host Endocytic Pathway is Essential for Plasmodium berghei Late Liver Stage Development. *Traffic*, *13*(10), 1351–1363. https://doi.org/https://doi.org/10.1111/j.1600-0854.2012.01398.x

Derbyshire, E. R., Mota, M. M., & Clardy, J. (2011). The Next Opportunity in Anti-Malaria Drug Discovery: The Liver Stage. *PLOS Pathogens*, *7*(9), e1002178-. https://doi.org/10.1371/journal.ppat.1002178

Gambarotto, D., Hamel, V., & Guichard, P. (2021). Chapter 4 - Ultrastructure expansion microscopy (U-ExM). In P. Guichard & V. Hamel (Eds.), *Methods in Cell Biology* (Vol. 161, pp. 57–81). Academic Press. https://doi.org/https://doi.org/10.1016/bs.mcb.2020.05.006

Gambarotto, D. et al. (2019). Imaging cellular ultrastructures using expansion microscopy (U-ExM). *Nature Methods*, *16*(1), 71–74. https://doi.org/10.1038/s41592-018-0238-1

Gao, R., Asano, S. M., & Boyden, E. S. (2017). Q&A: Expansion microscopy. *BMC Biology*, *15*(1), 50. https://doi.org/10.1186/s12915-017-0393-3

Heintzmann, R., & Ficz, G. (2006). Breaking the resolution limit in light microscopy. *Briefings in Functional Genomics*, *5*(4), 289–301. https://doi.org/10.1093/bfgp/ell036

Kaiser, G., De Niz, M., Burda, P.-C., Niklaus, L., Stanway, R. L., & Heussler, V. (2017). Generation of transgenic rodent malaria parasites by transfection of cell culture-derived merozoites. *Malaria Journal*, *16*(1), 305. https://www.unboundmedicine.com/medline/citation/28764716/Generation_of_transgenic_rodent_malaria_parasites_by_transfection_of_cell_culture_derived_merozoites_

Liffner, B., & Absalon, S. (2021). Expansion Microscopy Reveals Plasmodium falciparum Blood-Stage Parasites Undergo Anaphase with A Chromatin Bridge in the Absence of Mini-Chromosome Maintenance Complex Binding Protein. *Microorganisms*, *9*(11). https://doi.org/10.3390/microorganisms9112306

Mota, M. M., Pradel, G., Vanderberg, J. P., Hafalla, J. C. R., Frevert, U., Nussenzweig, R. S., Nussenzweig, V., & Rodríguez, A. (2001). Migration of Plasmodium Sporozoites Through Cells Before Infection. *Science*, *291*(5501), 141–144. https://doi.org/10.1126/science.291.5501.141

Niklaus, L., Agop-Nersesian, C., Schmuckli-Maurer, J., Wacker, R., Grünig, V., & Heussler, V. T. (2019). Deciphering host lysosome-mediated elimination of Plasmodium berghei liver stage parasites. *Scientific Reports*, *9*(1), 7967. https://doi.org/10.1038/s41598-019-44449-z

Plowe, C. V. (2022). Malaria chemoprevention and drug resistance: a review of the literature and policy implications. *Malaria Journal*, *21*(1), 104. https://doi.org/10.1186/s12936-022-04115-8

Rankin, K. E., Graewe, S., Heussler, V. T., & Stanway, R. R. (2010). Imaging liver-stage malaria parasites. *Cellular Microbiology*, *12*(5), 569–579. https://doi.org/https://doi.org/10.1111/j.1462-5822.2010.01454.x

Rashpa, R., & Brochet, M. (2022). Expansion microscopy of Plasmodium gametocytes reveals the molecular architecture of a bipartite microtubule organisation centre coordinating mitosis with axoneme assembly. *PLOS Pathogens*, *18*(1), e1010223-. https://doi.org/10.1371/journal.ppat.1010223

Roques, M., Bindschedler, A., Beyeler, R., & Heussler, V. T. (2023). Same, same but different: Exploring Plasmodium cell division during liver stage development. *PLOS Pathogens*, *19*(3), e1011210-. https://doi.org/10.1371/journal.ppat.1011210

Schindelin, J., et al. (2012). Fiji: an open-source platform for biological-image analysis. *Nature Methods*, *9*(7), 676–682. https://doi.org/10.1038/nmeth.2019

Snow, R. W., Guerra, C. A., Noor, A. M., Myint, H. Y., & Hay, S. I. (2005). The global distribution of clinical episodes of Plasmodium falciparum malaria. *Nature*, *434*(7030), 214–217. https://doi.org/10.1038/nature03342

Tavares, J., Formaglio, P., Thiberge, S., Mordelet, E., van Rooijen, N., Medvinsky, A., Ménard, R., & Amino, R. (2013). Role of host cell traversal by the malaria sporozoite during liver infection. *Journal of Experimental Medicine*, *210*(5), 905–915. https://doi.org/10.1084/jem.20121130

Tillberg, P. W. et al. (2016). Protein-retention expansion microscopy of cells and tissues labeled using standard fluorescent proteins and antibodies. *Nature Biotechnology*, *34*(9), 987–992. https://doi.org/10.1038/nbt.3625

Tse, E. G., Korsik, M., & Todd, M. H. (2019). The past, present and future of anti-malarial medicines. *Malaria Journal*, *18*(1), 93. https://doi.org/10.1186/s12936-019-2724-z

Vaughan, A. M., & Kappe, S. H. I. (2017). Malaria Parasite Liver Infection and Exoerythrocytic Biology. *Cold Spring Harbor Perspectives in Medicine*, *7*(6), a025486. https://doi.org/10.1101/cshperspect.a025486

Venugopal, K., Hentzschel, F., Valkiūnas, G., & Marti, M. (2020). Plasmodium asexual growth and sexual development in the haematopoietic niche of the host. *Nature Reviews Microbiology*, *18*(3), 177–189. https://doi.org/10.1038/s41579-019-0306-2

White, N. J. (2004). Antimalarial drug resistance. *The Journal of Clinical Investigation*, *113*(8), 1084–1092. https://doi.org/10.1172/JCI21682

WHO. (2021). *World malaria report 2021*.

Figures and Table

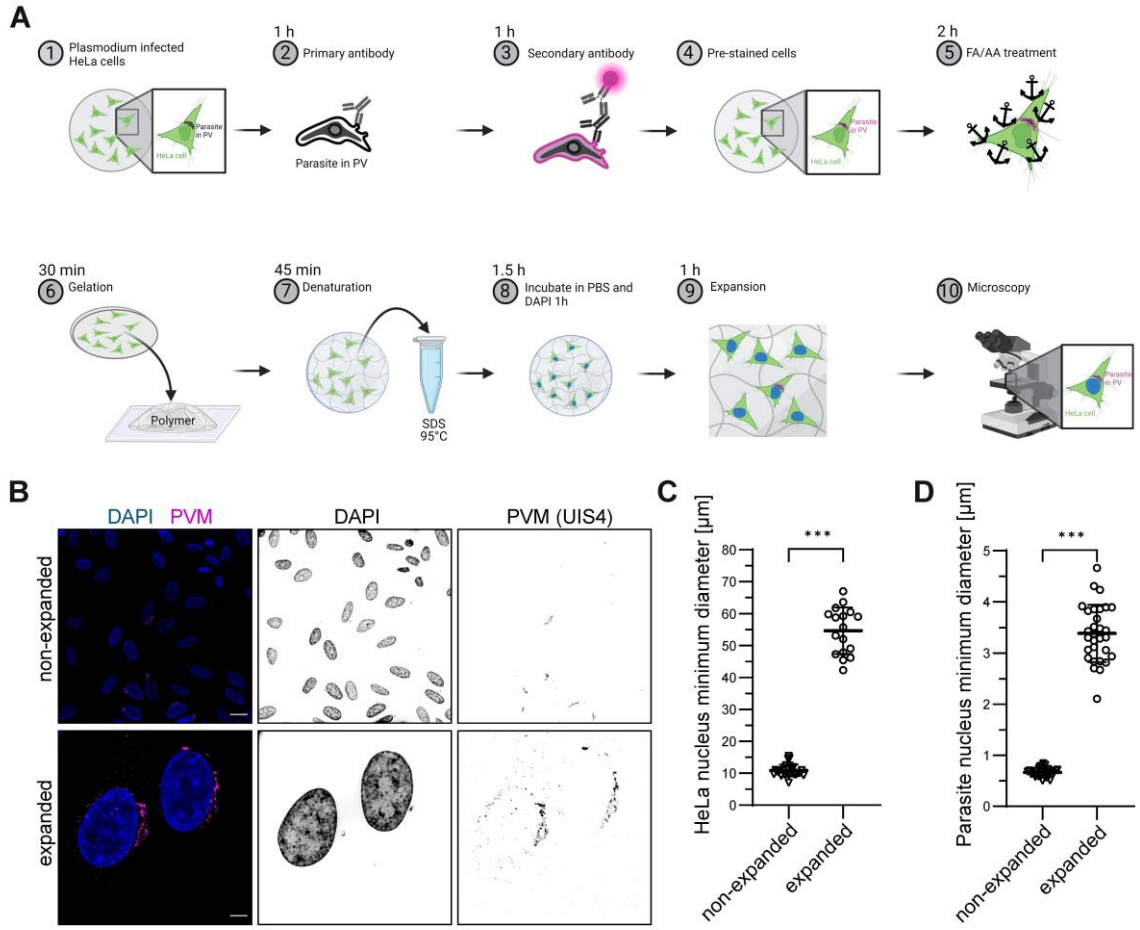

Fig. 1. Pre-gelation staining expansion microscopy (PS-ExM) workflow to study *Plasmodium* liver stage and expansion factor quantification. (A) Overview of the procedure. Briefly, prior to the experiment, HeLa cells are seeded onto a coverslip and infected with sporozoites the next day (1). After fixation and permeabilization, the cells are stained with primary (2) and secondary antibodies (3). The pre-stained cells (4) are subsequently fixed with formaldehyde (FA) and anchors are introduced with acrylamide (AA) (5), before the cells are embedded into a hydrogel (6) and the protein denatured in an SDS-containing buffer (7). The gel is washed with PBS before staining the nuclear DNA with DAPI (8). Cells are investigated with wide field microscopy (10) after expanding the gel (9). Overview created with BioRender.com **(B)** Expansion of infected HeLa cells six hours post-

infection. DNA was stained with DAPI (blue) and the parasitophorous vacuole membrane (PVM, magenta) with UIS4 (up-regulated in infective sporozoites gene 4) antibody staining. The expansion factor was determined based on DAPI staining. Scale bars = 20 µm. **(C)** Minimal nuclear diameter for non-expanded (n = 27) and expanded (n = 17) HeLa cells. The expansion factor of HeLa cell nuclei measured 5-fold. **(D)** Minimal nuclear diameter for non-expanded (n = 30) and expanded (n = 30) parasites. The expansion factor of parasite nuclei measured 5.1-fold. Data points are shown as individual values and mean ± SD. Statistical analysis was performed using student's t-test: *** P <0.001; ** P <0.01; * P <0.05.

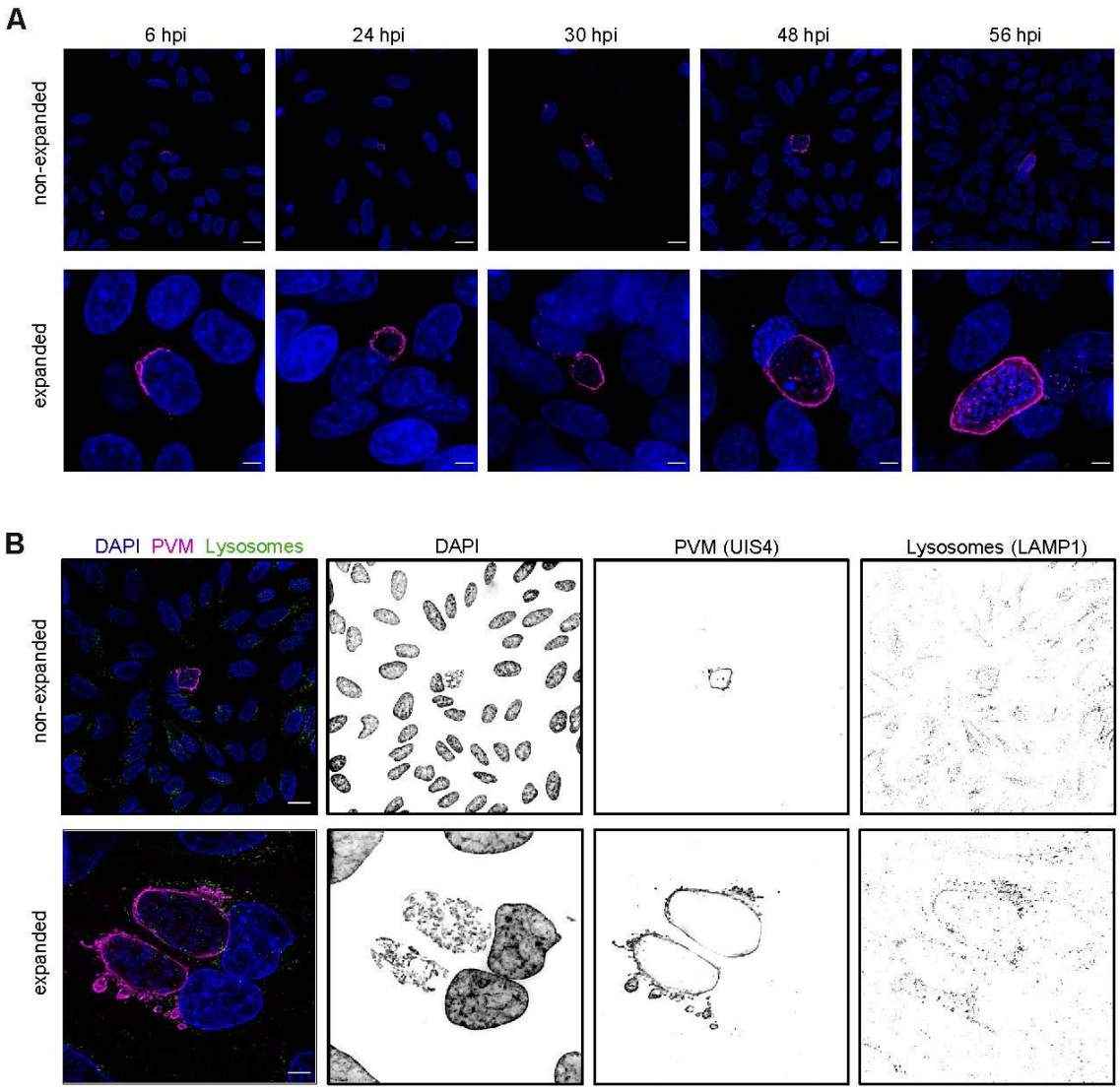

Fig. 2. Pre-gelation staining expansion microscopy (PS-ExM) of entire *Plasmodium* liver stage development. (A) PS-ExM of entire *Plasmodium* liver stage development. Non-expanded (top row) and expanded (lower row) cells stained with DAPI to visualise nuclei (blue) and antibody staining of UIS4 (up-regulated in infective sporozoites gene 4) to visualise the parasitophorous vacuole membrane (PVM, magenta) at different time points (hours post-infection, hpi). **(B)** Visualisation of parasite and host proteins in PS-ExM 48 hours post-infection. DNA DAPI staining is shown in blue. Antibody staining was performed to visualise the parasite protein UIS4, which stains the PVM (magenta) and LAMP1 (lysosome-associated membrane protein 1) staining host lysosomes (green). Scale bars = 20 µm.

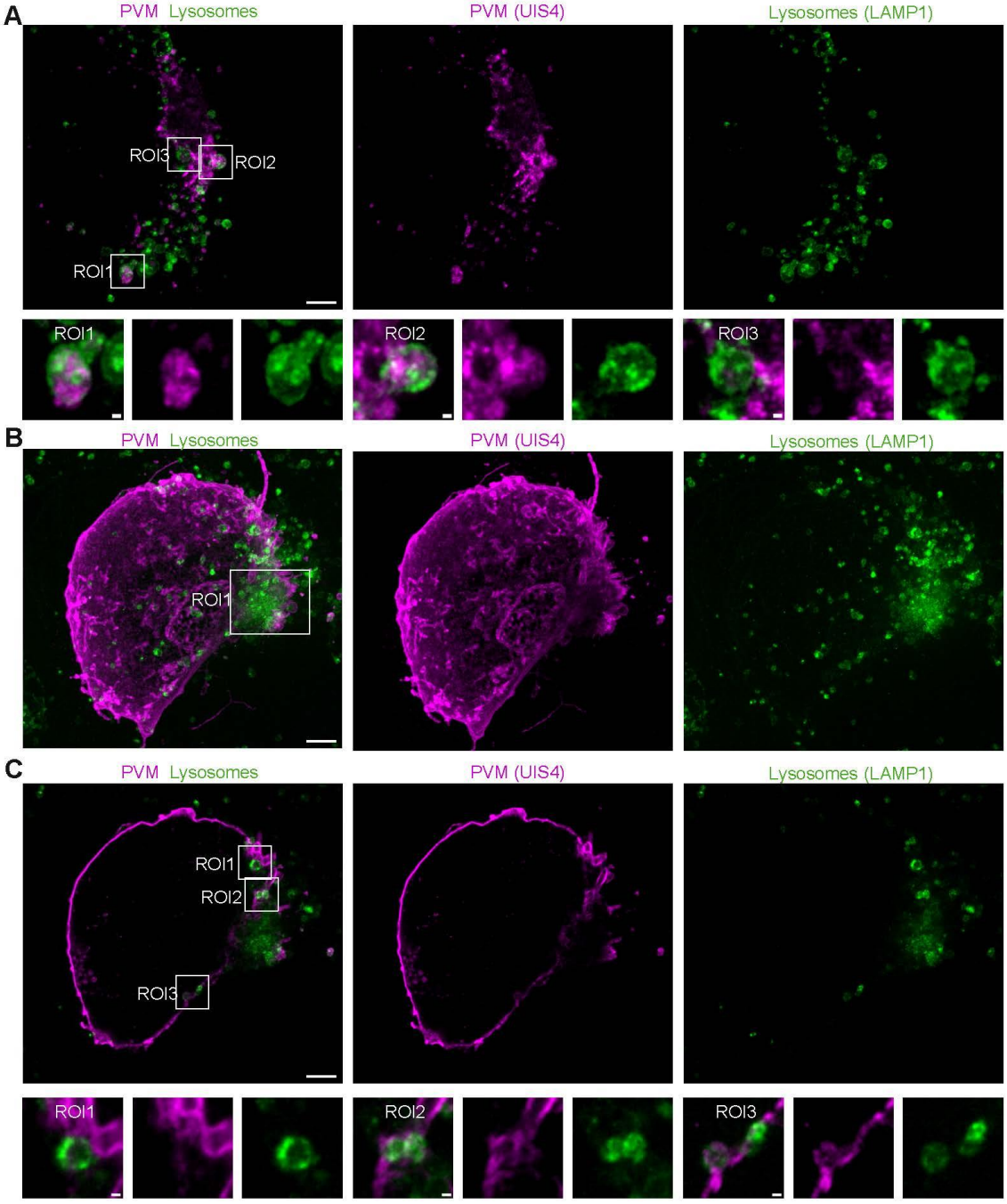

Fig. 3. PS-ExM sheds light on the interaction between parasite PVM and host lysosomes. **(A)** Representative images of PS-ExM-expanded HeLa cells infected with *Plasmodium* sporozoites. The cells were PFA fixed at 6 hpi and stained with anti-LAMP1 (green) and anti-UIS4 (magenta). ROI1, ROI2, and ROI3 show how parts of the PVM were engulfed by lysosomal vesicles. **(B and C)** Images of expanded HeLa cells that were infected with *Plasmodium* sporozoites and fixed with

PFA at 48 hpi. Lysosomes were stained with anti-LAMP1 (green) and the PVM with anti-UIS4 (magenta). **(B)** Maximum z-projection of the confocal images. ROI1 shows how the host cell lysosomes are accumulated in close proximity to the parasite tubo-vesicular network (TVN). **(C)** Single-plane image of the confocal images shown in **(B)**. ROI1 to 3 show in detail how lysosomes get attached (ROI1), fused (ROI2), and become integrated into the parasite PVM (ROI3). All the images were acquired with the Nikon Ti 2 Crest V3 in spinning disc mode. ROI = Region of Interest; scale bars = 10 µm for the main images and 1 µm for the ROIs.

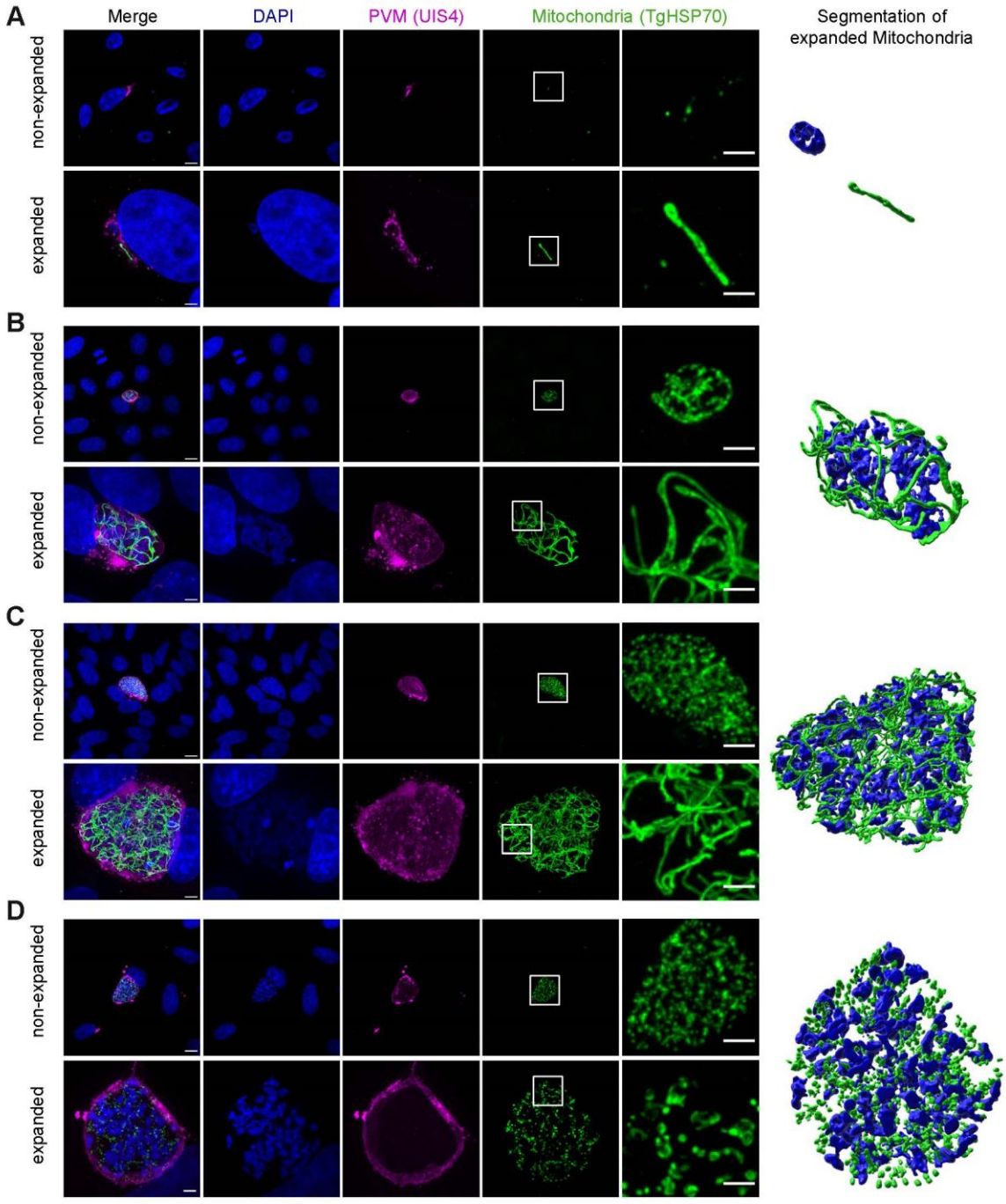

Fig. 4. Pre-gelation staining expansion microscopy (PS-ExM) of *Plasmodium* liver stage parasites allows visualisation of parasite mitochondria. (A)-(C) Confocal images of parasite mitochondria in infected HeLa cells fixed with PFA at 6, 48, and 56 hours post-infection, respectively. DNA was stained with DAPI and is shown in blue. Antibody staining was performed to visualise the parasitophorous

vacuole membrane (UIS4, magenta) and parasite mitochondria (HSP70, green). Non-expanded samples are in the top row, and pre-gelation staining expansion microscopy images are at the bottom. Scale bars = 10 μm for the main images and 5 μm for the ROIs. The mitochondrial network and parasite nuclei were segmented with Imaris software.

Table 1. Comparison between the original post-gelation staining protocol and the modified version for pre-expansion-stained specimens presented in this publication (PS-ExM).

Property	Post-gelation staining U-ExM (Gambarotto et al., 2019, 2021)	Pre-gelation staining ExM PS-ExM
Antibody incubation times	Primary antibody: 3 h Secondary antibody: 2.5 h	Primary and secondary antibody: each 1 h
Fixation/Anchoring (FA/AA treatment) time	5 h	2 h
Gelation at 37°C	1 h	30 min
Denaturation	1 h 45 min	45 min
DAPI staining	During secondary AB incubations (2.5 h)	Separate staining after gelation (1 h)
Lysosome staining	Poor	Good
PVM	Good, but not complete	Good
Tubulin staining	Poor	Good
Expansion	Isotropic (4.5 x)	Isotropic (5 x)
Amount of gel stained	1/8	Whole gel
Non-expanded control	Performed separately (different protocol for staining compared to U-ExM)	Performed alongside (same protocol as staining for U-ExM)

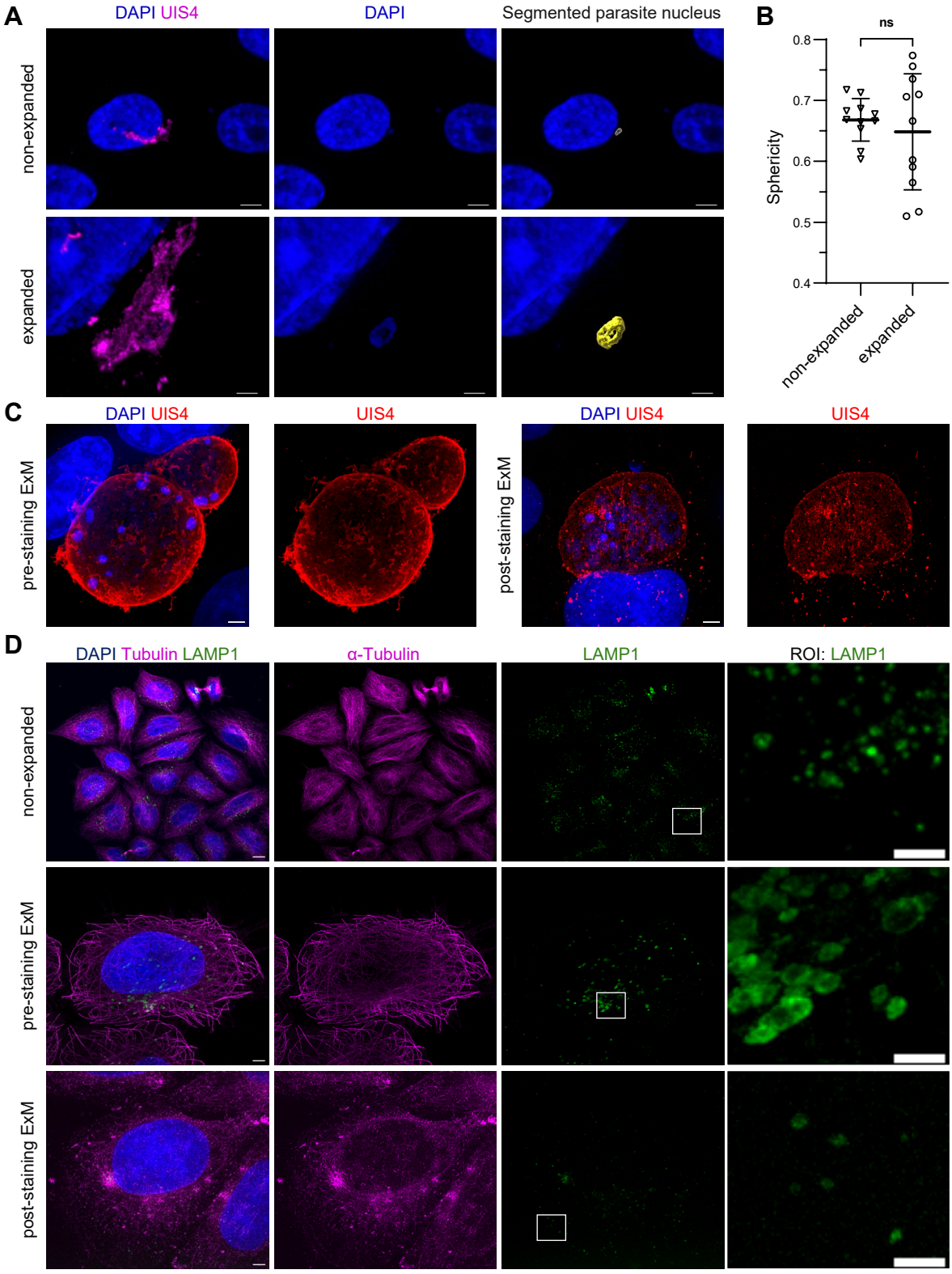

Fig. S1. PS-ExM results in isotropic expansion and preservation of epitope. **(A)** z-stack confocal images of non-expanded and expanded fixed infected cells at 6 hpi. The PVM was stained with anti-UIS4 (magenta), and the host cell and parasite nuclei were stained with DAPI (blue). To determine the isotropicity of the PS-ExM protocol, the nucleus sphericity was measured using the 3D and 4D image analysis software Imaris. Briefly, the parasite DAPI signal was used to compute the 3D isosurface and measure the sphericity. A nucleus with an exact spherical shape will have a sphericity value of 1, which is the maximum. **(B)** Non-expanded (n = 11) and PS-ExM-expanded (n = 11) nuclei exhibit an average sphericity of 0.67 and 0.65, respectively, with no significant difference. Image scale bar = 5 µm. Data points are shown as individual values and mean ± SD. Statistical analysis was performed using the student's t-test: *** P <0.001; ** P <0.01; * P <0.05. **(C)** Comparison between PVM epitope preservation in the pre-staining ExM and the post-staining ExM protocols. The parasite PVM was stained with anti-UIS4 (red) and the parasite and HeLa cell nuclei with DAPI (blue). Image scale bars = 10 µm. **(D)** Comparison of epitope preservation in the non-expanded, pre-staining ExM, and post-staining ExM HeLa cells. The host cell's microtubules were stained with anti-α-tubulin (magenta), lysosomes with anti-LAMP1 (green), and cell nuclei with DAPI (blue). Image scale bar = 10 µm.

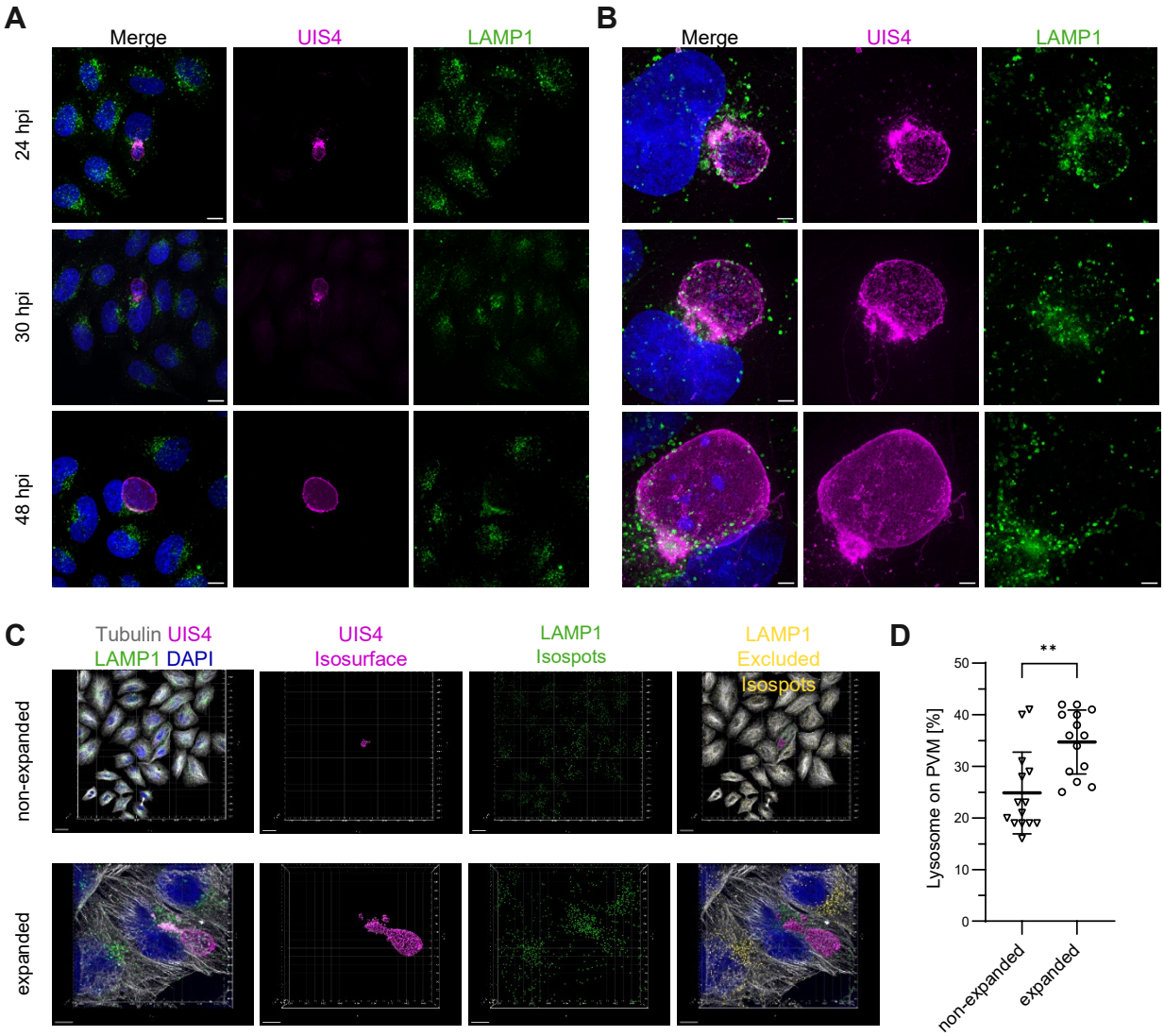

Fig. S2. PS-ExM improves the quantification of the host lysosome and parasite PVM interaction. (A and B) Confocal images of infected HeLa cells. The HeLa cells were infected with *Plasmodium* sporozoites and fixed at different time points (24 hpi, 30 hpi, and 48 hpi). Cells were stained with anti-LAMP1 (green), anti-UIS4 (magenta), and DAPI for the host cell and parasite nuclei (blue). The images show how the host cell lysosome interacts with the parasite during the liver stage development of the parasite until schizogony. Image scale bar =10 µm. **(A)** Non- expanded cells. **(B)** Expanded cells. **(C)** To quantify the lysosome-PVM interaction, the 3D and 4D image analysis software Imaris was used, as described in the method section. The 24 hpi cells were used for the quantification. Briefly, the anti-LAMP1 (green) signal was used to compute 3D lysosome isospots, and the anti-UIS4 signal (magenta) was used to compute the PVM 3D isosurface. The anti-α-tubulin signal (grey) was used to delimit a single cell border and exclude the LAMP1 signal of non-infected cells (excluded isospots in yellow). The images show non-expanded and expanded cells. Scale bar = 20 µm. **(D)** Percentage of attached lysosomes to the PVM per infected cell in non-expanded (n = 14) and expanded (n = 14) cells. On average, 35% of the host lysosome was fused to the PVM (0 µm distance to the PVM) in the expanded cells and 25% in the non-expanded cells. Data points are shown as individual values and mean ± SD. Statistical analysis was performed using the student's t-test: *** P <0.001; ** P <0.01; * P <0.05.

Table S1. Overview of antibodies and chemicals used for the immunofluorescence assay.

Antibody/Chemical	Company/Provider	Catalogue Number	PS-ExM dilution	Post-staining ExM dilution
anti-UIS4 rabbit	P-Sinnis, Baltimore		1:1000	1:500
anti-UIS4 chicken	Produced by Proteogenix in 2021		1:1000	
anti-LAMP1 mouse	Developmental Hybridoma Bank, clone H4A3		1:1000	1:500
anti-TgHSP70 rabbit	Gift from Dominique Soldati Favre		1:500	
anti-α-tubulin guinea pig	Geneva Antibody Facility	AA345	1:200	1:125
anti-rabbit ATTO 647	SIGMA	40839	1:1000	1:500
anti-mouse Alexa Fluor 488	Invitrogen Molecular Probes	A11001	1:1000	1:500
anti-guinea pig Alexa Fluor 594	Invitrogen Molecular Probes	A11076	1:1000	1:500
anti-chicken Alexa Fluor 594	Invitrogen Molecular Probes	A11042	1:500	
TritonX 100	Fluka Chemie	T8787	0.05%	
ProLong™ Gold antifade reagent	Invitrogen	P36930		
DAPI (100 µg ml^{-1})	SIGMA	D9542	1:100	

Table S2. Overview of chemicals used for expansion microscopy: for each chemical, the abbreviation (abbr.), company, catalogue number, amount, storage and additional comments are given.

Chemical	Abbr.	Company	Catalogue Number	Amount	Comments	Storage
Formaldehyde 36.5–38%	FA	SIGMA	F8775	25 ml	TOXIC! Ready to use. Use under the hood.	RT
Acrylamide 40%	AA	SIGMA	A4058	100 ml	TOXIC! Ready to use. Use under the hood.	4°C
N,N-methylene-bisacrylamide 2%	BIS	SIGMA	M1533	25 ml	TOXIC! Ready to use. Use under the hood.	4°C
Sodium Acrylate	SA	SIGMA	408220	25 g	TOXIC! Use powder under the hood.	powder at -20°C, 38% solution at 4°C in the dark!
Ammonium persulfate	APS	Thermo-Fisher	17874		Make 10% aliquots (à 20 µl)	aliquots -20°C
Tetramethyl-ethylene-diamine	TEMED	Thermo-Fisher	17919		Make 10% aliquots (à 20 µl)	aliquots -20°C
Poly-D-Lysine		Gibco	A38904	100 ml	Ready to use	4°C
4′,6-diamidino-2-phenylindole	DAPI	SIGMA	D9542	5 mg	Aliquots with 5 mg ml^{-1} (à 10µl)	stock and aliquots at -20°C in the dark
Propyl gallate		SIGMA	02370		Powder	RT

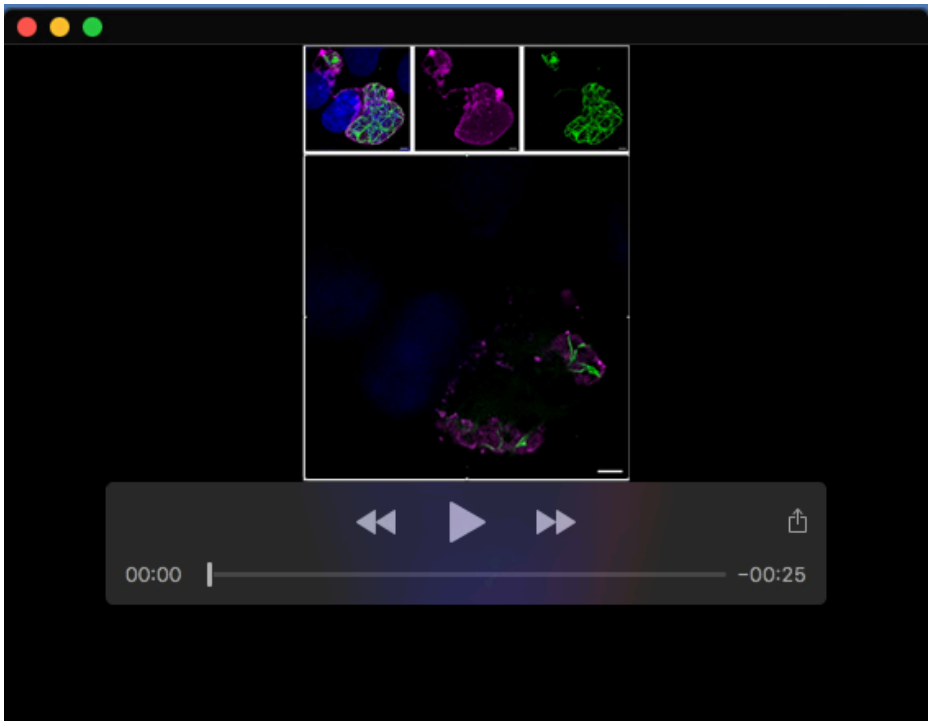

Movie 1. PS-ExM of the parasite mitochondrial network stained with anti-TgHSP70 (green), PVM stained with anti-UIS4 (magenta), and nuclei stained with DAPI (blue).